ISSN 2176-5480

22nd International Congress of Mechanical Engineering (COBEM 2013)
November 3-7, 2013, Ribeirão Preto, SP, Brazil

AN EFFICIENT STRATEGY TO INTRODUCE FIBRES IN FEM LAMINATED PLATE ANALYSIS

Maria do Socorro Martins Sampaio
São Carlos School of Engineering, University of São Paulo, Brazil
ssampaio@sc.usp.br

Rodrigo Ribeiro Paccola
São Carlos School of Engineering, University of São Paulo, Brazil
rpaccola@sc.usp.br

Humberto Breves Coda
São Carlos School of Engineering, University of São Paulo, Brazil
hbcoda@sc.usp.br

Abstract. *In this study we develop a geometrically non-linear plate FEM formulation to analyze laminated plates including straight or curved fibers inside the domain without increasing the number of degrees of freedom. Moreover the position of fibers are free from the plate discretization and the coupling is done in an automatic way, i.e., the fiber mesh generator is totally independent of the plate mesh generator. The formulation is based on the positional FEM technique in which finite rotations are considered without the use of Euler-Rodriguez or quaternion formulae. Results are compared with a homogenized laminated shell formulation proving the good behavior and future possibilities of the proposed formulation.*

Keywords: *finite element method, laminated plates, geometrical nonlinearity, fibre-reinforced laminates.*

1. INTRODUCTION

As well known, structures made of more one material to take the advantage of those material´s complementary characteristics, for example those ones made by fibre-reinforced composites. By other hand, the continuous improvement of materials strength and stiffness leads to the design of slender and flexible structures generally undergoing large displacements. To analyze structures with these characteristics laminated plates and shells finite elements have been shown to be an excellent tool.

Usually, fibre reinforced solids are analyzed by homogeneous analog wich makes difficult to identify the contact stresses between fibres and matrix. There are many interesting techniques proposing the fibre-matrix coupling in literature, see for example (Radtke *et al.*, 2011; Radtke *et al.*, 2010a; Radtke *et al.*, 2010b; Hettich *et al.*, 2008; Chudoba *et al.*, 2009; Oliver *et al.*, 2008; Melenk and Babuska, 2006; Schlanger and van Mier, 1992; Bolander and Saito, 1997).

In this paper we propose a way to represent short or long fibres immersed in laminated plates or shells by means of curved finite elements without increasing the number of degrees of freedom. We use the total Lagrangian description and the Saint-Venant-Kirchhoff constitutive law (Ciarlet, 1993; Ogden, 1984) is chosen to model the material behavior. To solve the resulting geometrical nonlinear problem we adopt the Principle of Stationary Total Potential Energy (Tauchert, 1974). From this principle we find the nonlinear equilibrium equations and the Newton-Raphson iterative procedure (Luenberg, 1989) used to solve the nonlinear system. External loads are conservative and incrementally applied.

To present the proposed formulation we organize the paper as follows. Section 2 describes some concepts about strain energy function used in this paper to model orthotropic media; in Section 3 the Reissner-Mindlin kinematic used to model laminate orthotropic plates or shells is provided; in Section 4 we present the kinematics used to describes the any order fibre finite elements as well its internal force vector and the matrix hessian; in Section 5 the spreading strategy that makes possible a complete analysis of any order fibres into laminated plate or shell finite elements without increasing the number of degrees of freedom is introduced; in Section 6 the general nonlinear solution process is described; Section 7 presents the numerical examples validating the proposed formulation and finally, conclusions are presented in Section 8.

2. STRAIN ENERGY FUNCTION FOR ORTHOTROPIC MEDIA

To derive the formulation proposed in this paper we adopt the Saint-Venant-Kirchhoff strain energy function, whose the Green strain and the second Piola-Kirchhhoff stress are the conjugate variables.

The Green strain tensor is derived directly from the gradient of the deformation function, represented by letter A, given as follows

ISSN 2176-5480

$$A_{ij} = \frac{\partial f_i}{\partial x_j} = f_{i,j} \tag{1}$$

where f_i is the deformation function. One writes the Green strain as

$$E_{ij} = \frac{1}{2}\left[A_{ki} A_{kj} - \delta_{ij} \right] = \frac{1}{2}\left[C_{ij} - \delta_{ij} \right] \tag{2}$$

in which index notation is adopted. The second order tensors C_{ij} and δ_{ij} are the right Cauchy-Green stretch and the Kroenecker delta, respectively. The quadratic strain energy per unit of initial volume, Saint-Venant-Kirchhoff, is given by

$$u_S = \frac{1}{2} E_{ij} D_{ijkl} E_{kl} \tag{3}$$

resulting in a linear elastic constitutive relation between the second Piola-Kirchhoff stress and Green strain, i.e.:

$$S_{ij} = \frac{\partial u_s}{\partial E_{ij}} = D_{ijkl} E_{kl} \tag{4}$$

The fourth order tensor D_{ijkl} is the usual linear orthotropic constitutive tensor (Hyer, 1997). The hole strain energy stored in a body is written for the reference volume V_0 as

$$U_S = \int_{V_0} u_S \, dV_0 = \int_{V_0} \frac{1}{2} E_{ij} D_{ijkl} E_{kl} \, dV_0 \tag{5}$$

The first and the second derivative of the strain energy in terms of a general set of nodal parameters Y_j are given, respectively, by

$$\frac{\partial U_s}{\partial Y_j} = \int_{V_0} \frac{\partial u_s}{\partial Y_j} dV_0 = \int_{V_0} D_{\alpha\beta im} E_{im} \frac{\partial E_{\alpha\beta}}{\partial Y_j} dV_0 \tag{6}$$

$$\frac{\partial^2 U_s}{\partial Y_k \partial Y_j} = \int_{V_0} \frac{\partial^2 u_s}{\partial Y_k \partial Y_j} dV_0 = \int_{V_0} \frac{\partial}{\partial Y_k} \left(D_{\alpha\beta im} E_{im} \frac{\partial E_{\alpha\beta}}{\partial Y_j} \right) dV_0 \tag{7}$$

3. REISSNER-MINDLIN KINEMATIC FOR LAMINATED PLATES OR SHELLS

First, we present a kinematic description for homogeneous shell and then a generalization for a laminate orthotropic shell is provided.

In this study we call pure Reissner-Mindlin kinematic based on position and unconstrained vector the one presented by (Coda and Paccola, 2007) and depicted in Fig. 1. The shell, or plate, can change thickness and naturally present distortion along transverse direction.

From Fig. 1, a generic point x at the initial configuration is written as a function of a point x^m at the reference surface and a generic vector g^0. Using the same procedure, a generic point y at the current configuration is written as a function of a point y^m at the reference surface and a unconstrained generic vector g^1. These variables are written as function of non-dimensional coordinates, ξ_i, generating the initial f^0 and the current f^1 mappings, as well their corresponding gradients, A^0 and A^1, written as

$$f_i^0 = x_i = \phi_\ell(\xi_1, \xi_2) X_{\ell i} + \frac{h_0}{2} \xi_3 \phi_\ell(\xi_1, \xi_2) N_{i\ell}^0 \tag{8}$$

ISSN 2176-5480

$$f_i^1 = y_i = \phi_\ell(\xi_1,\xi_2)Y_{\ell i} + \frac{h_0}{2}\xi_3\,\phi_\ell(\xi_1,\xi_2)G_{i\ell} \tag{9}$$

$$g_i^0 = \frac{h_0}{2}\xi_3\phi_\ell(\xi_1,\xi_2)N_{i\ell}^0 \tag{10}$$

$$g_i^1 = \frac{h_0}{2}\xi_3\ \phi_\ell(\xi_1,\xi_2)G_{i\ell} \tag{11}$$

$$A_{ij}^0 = \frac{\partial f_i^0}{\partial \xi_j} = f_{i,j}^0\ ,\ A_{ij}^1 = \frac{\partial f_i^1}{\partial \xi_j} = f_{i,j}^1 \tag{12}$$

in which ϕ_ℓ is a shape function (third order in this study) related to node ℓ and $X_{\ell i}$, $N_{i\ell}^0$, $Y_{\ell i}$ and $G_{i\ell}$ are nodal parameters. The value h_0 is the initial thickness of the shell, see (Coda and Paccola, 2007) for more details.

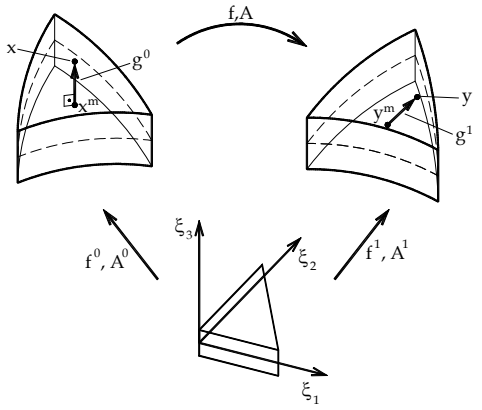

Figure 1. Position vectors for kinematic description

The deformation function f is not explicitly written; however its gradient is achieved from A^0 and A^1, as

$$A = A^1 \cdot (A^0)^{-1} \tag{13}$$

To avoid volumetric and shear locking from usual homogeneous or laminate shell formulations (Coda and Paccola, 2008; Coda *et al.*, 2013), a linear rate of thickness variation given by

$$T(\xi_1,\xi_2) = \phi_\ell(\xi_1,\xi_2)\overline{T}_\ell \tag{14}$$

is introduced in Eq. (9) as follows

$$f_i^1 = y_i = \phi_\ell(\xi_1,\xi_2)Y_{\ell i} + \frac{h_0}{2}\left[\xi_3 + \phi_\ell(\xi_1,\xi_2)\overline{T}_\ell\ \xi_3^2\right]\phi_\ell(\xi_1,\xi_2)G_{i\ell} \tag{15}$$

The inexistence of finite rotation description allows the understanding of laminate kinematic by a simple two dimensional representation depicted in Fig. 2.

From the new variables introduced in Fig. 2, the new formulae for the initial and current mappings are achieved substituting $\frac{h_0}{2}\xi_3$ by $\left(d^{lam} + \frac{h_0^{lam}}{2}\xi_3\right)$ into Eqs. (8), (9) and (15), respectively, as

$$f_i^{0lam} = \phi_\ell(\xi_1,\xi_2)X_{\ell i} + \left(d^{lam} + \frac{h_0^{lam}}{2}\xi_3\right)\phi_\ell(\xi_1,\xi_2)N_{i\ell}^0 \tag{16}$$

ISSN 2176-5480

$$f_i^1 = y_i = \phi_\ell(\xi_1,\xi_2)Y_{\ell i} + \left(d^{lam} + \frac{h_0^{lam}}{2}\xi_3 \right)\phi_\ell(\xi_1,\xi_2)\bar{G}_{i\ell} \tag{17}$$

$$f_i^{1\,lam} = \phi_\ell(\xi_1,\xi_2)Y_{\ell i} + \left[\left(d^{lam} + \frac{h_0^{lam}}{2}\xi_3 \right) + \phi_\ell(\xi_1,\xi_2)\bar{T}_\ell \left(d^{lam} + \frac{h_0^{lam}}{2}\xi_3 \right)^2 \right]\phi_k(\xi_1,\xi_2)\bar{G}_{ik} \tag{18}$$

in which the superscript lam indicates the considered lamina, d^{lam} is the distance from the reference surface to the center of the considered lamina following direction g_i^0 at initial configuration and h_0^{lam} is its initial thickness. The rate of thickness variation of each lamina $\bar{T}_\ell^{lam}$ can be recovered from its average representation $\bar{T}_\ell$ by $\bar{T}_\ell^{lam} = (h_0^{lam}/2)\bar{T}_\ell$.

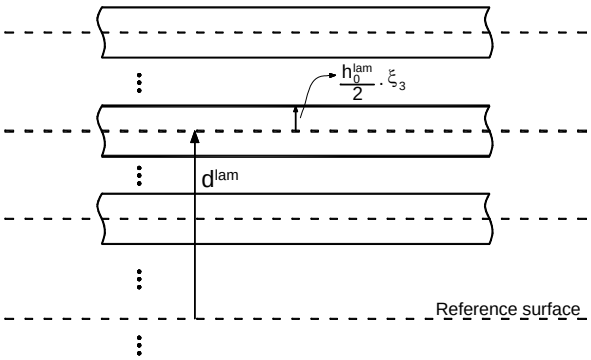

Figure 2. Kinematic description for laminate shells

The derivatives of mapping f_i^{1lam} regarding the non-dimensional variables, constitute the gradient A_{ij}^{1lam} while the same procedure imposed on f_i^{0lam} results A_{ij}^{0lam}, see Eq. (12).

4. ELASTIC FIBRE REINFORCEMENT: KINEMATICS AND ENERGY CONSIDERATIONS

In this section we present the kinematics description and some energy strain considerations used to obtain the internal force and the matrix hessian of a general curved fibre of any order. In next section we will describe the strategy used to introduce the fibre energy in the composite solution without increasing the number of degrees of freedom. To guaranty total adherent fiber-matrix coupling it is necessary to adopt high order fibre elements (Sampaio *et al*., 2013).

Figure 2 shows the non-deformed initial configuration B_0, the current configuration B and a non-dimensional auxiliary configuration B_1 for the curved fibre finite element of any order.

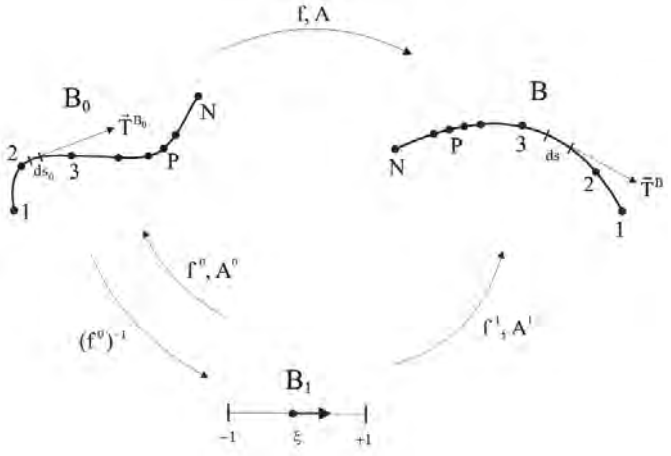

Figure 3.: Mapping of the fibre finite element in initial and current configurations

ISSN 2176-5480

The initial configuration B_0 whose points have coordinates x_i is mapped from the dimensionless space B_1 with coordinates ξ using shape functions of any order, $\phi_P(\xi)$, and by the coordinates of nodes P in the initial configuration, X_i^P, such as:

$$x_i = f_i^0 = \phi_P(\xi) X_i^P \tag{19}$$

The current configuration B is mapped from the dimensionless space B_1 by:

$$y_i = f_i^1 = \phi_P(\xi) Y_i^P \tag{20}$$

where y_i are the coordinates of points in the current configuration B and Y_i^P are the current coordinates of fiber nodes in the current configuration. In Eqs. (19) and (20) index $P = 1,...,N$ and $i = 1,...,3$ represent, respectively, the fiber finite element nodes and coordinate directions.

The tangent vector of the fiber and its modulus are calculated at the initial configuration as

$$T_i^{B_0} = \frac{d\phi_P(\xi)}{d\xi} X_i^P \text{ and } \left|\vec{T}^{B_0}\right|^2 = \left(\frac{d\phi_P(\xi)}{d\xi} X_1^P\right)^2 + \left(\frac{d\phi_P(\xi)}{d\xi} X_2^P\right)^2 + \left(\frac{d\phi_P(\xi)}{d\xi} X_3^P\right)^2 \tag{21}$$

It is important to mention that $\left|\vec{T}^{B^0}\right|$ is the differential Jacobian of f_i^0. For the current configuration one finds

$$T_i^B = \frac{d\phi_P(\xi)}{d\xi} Y_i^P \text{ and } \left|\vec{T}^B\right|^2 = \left(\frac{d\phi_1(\xi)}{d\xi} Y_1^P\right)^2 + \left(\frac{d\phi_1(\xi)}{d\xi} Y_2^P\right)^2 + \left(\frac{d\phi_1(\xi)}{d\xi} Y_3^P\right)^2 \tag{22}$$

From the tangent vector modulus, Eqs. (21) and (22), the one-dimensional Green strain is written as

$$E = \frac{1}{2}\left(\frac{\left|\vec{T}^B\right|^2 - \left|\vec{T}^{B_0}\right|^2}{\left|\vec{T}^{B_0}\right|^2}\right) \tag{23}$$

Using the Saint-Venant-Kirchhoff constitutive law, one writes the specific strain energy at a point of the fiber as

$$u_f(\xi) = \frac{1}{2}\mathscr{E}\left[E(\xi)\right]^2 \tag{24}$$

where $\mathscr{E}$ is the elastic modulus and $E(\xi)$ is the Green strain measure defined in Eq. (23).

The strain energy of a curved fiber is given by integrating Eq. (24) over its initial volume V_0 as:

$$U_f = \int_{V_0} u_f dV_0 \tag{25}$$

In order to proceed with the equilibrium analysis it is necessary to know the first derivative of strain energy regarding positions. Based on the energy conjugate concept the natural internal fiber force vector, $F_i^{j\,f\,int}$, related to node j and direction i is calculated regarding fiber parameters as

$$F_k^{j\,f\,int} = \frac{\partial U_f}{\partial Y_k^j} = \int_{V_0} \frac{\partial u_f}{\partial Y_k^j} dV_0 \tag{26}$$

The Hessian matrix components for the fibre element are obtained by the second derivative of the strain energy, i.e.:

ISSN 2176-5480

$$H^f_{kj\alpha\beta} = \frac{\partial^2 U_f}{\partial Y_k^j \partial Y_\alpha^\beta} = \int_{V_0^f} \frac{\partial^2 u_f}{\partial Y_k^j \partial Y_\alpha^\beta} dV_0^f = \int_{V_0^f} h^f_{kj\alpha\beta} dV_0^f \tag{27}$$

5. KINEMATICAL FIBRE-LAMINATED PLATE COUPLING

In this section we present the strategy used to introduce the fibres in the laminated plate or shell. We know that the strain energy stored in a laminate reinforced body is the sum of the strain energy stored in the matrix and fiber, that is

$$U = U_s + U_f \tag{28}$$

where U_s is the strain energy stored in the laminated plate or shell finite elements used to discretize the matrix and U_f is the strain energy stored in the fiber finite elements. From this expression we will derive the general internal force and the Hessian matrix considering the fibre and matrix contributions.

5.1 General internal force

The internal force at a node β following direction α, considering both fiber and matrix contributions is found by the conjugate energy concept, such as

$$\frac{\partial (U_S + U_f)}{\partial Y_\alpha^\beta} = \frac{\partial U_S}{\partial Y_\alpha^\beta} + \frac{\partial U_f}{\partial Y_\alpha^\beta} = \frac{\partial U_S}{\partial Y_\alpha^\beta} + \frac{\partial U_f}{\partial Y_i^P}\frac{\partial Y_i^P}{\partial Y_\alpha^\beta} = F_\alpha^{\beta S} + \frac{\partial Y_i^P}{\partial Y_\alpha^\beta} F_\alpha^{P f} = F_\alpha^{\beta int} \tag{29}$$

where Eq. (26) have been used and there is no summation over P.

5.2 Hessian Matrix

Proceeding in the same way as described for the calculation of internal forces, we develop the second derivative of strain energy of the reinforced finite element regarding the plate or shell nodal parameters, as follows

$$\frac{\partial^2 U}{\partial Y_\alpha^\beta \partial Y_\gamma^\xi} = \frac{\partial^2 \left(U_S + U_f\right)}{\partial Y_\alpha^\beta \partial Y_\gamma^\xi} = \int_{V_0} \frac{\partial^2 (u_S + u_f)}{\partial Y_\alpha^\beta \partial Y_\gamma^\xi} dV_0 = \int_{V_0} \frac{\partial^2 u_S}{\partial Y_\alpha^\beta \partial Y_\gamma^\xi} dV_0 + \int_{V_0^f} \frac{\partial^2 u_f}{\partial Y_\alpha^\beta \partial Y_\gamma^\xi} dV_0^f \tag{30}$$

The first integral at the last term of Eq. (30) is known, Eq. (7). However, it is necessary to observe that the kernel of the last integral is the specific strain energy of a fiber derived twice regarding the plate or shell nodal parameters. As Eq. (27) gives its value when derived regarding fiber parameters one has to apply the chain rule twice over Eq. (30), that is

$$\frac{\partial^2 u_f}{\partial Y_\alpha^\beta \partial Y_\gamma^\xi} = h^f_{\omega\rho\omega\rho} \frac{\partial Y_\omega^{\rho f}}{\partial Y_\alpha^\beta}\frac{\partial Y_\omega^{\rho f}}{\partial Y_\gamma^\xi} + h^f_{\omega\rho\pi\eta} \frac{\partial Y_\omega^{\rho f}}{\partial Y_\alpha^\beta}\frac{\partial Y_\pi^{\eta f}}{\partial Y_\gamma^\xi} + h^f_{\pi\eta\omega\rho} \frac{\partial Y_\pi^{\eta f}}{\partial Y_\alpha^\beta}\frac{\partial Y_\omega^{\rho f}}{\partial Y_\gamma^\xi} + h^f_{\pi\eta\pi\eta} \frac{\partial Y_\pi^{\eta f}}{\partial Y_\alpha^\beta}\frac{\partial Y_\pi^{\eta f}}{\partial Y_\gamma^\xi} \tag{31}$$

where $\boldsymbol{h}^f$ is the fiber Hessian matrix kernel, Eq. (27). In Eq. (29) summation is not implyied.

Integrating Eq. (31) over fiber volume gives

$$\frac{\partial^2 U_f}{\partial Y_\alpha^\beta \partial Y_\gamma^\xi} = H^f_{\omega\rho\omega\rho} \frac{\partial Y_\omega^{\rho f}}{\partial Y_\alpha^\beta}\frac{\partial Y_\omega^{\rho f}}{\partial Y_\gamma^\xi} + H^f_{\omega\rho\pi\eta} \frac{\partial Y_\omega^{\rho f}}{\partial Y_\alpha^\beta}\frac{\partial Y_\pi^{\eta f}}{\partial Y_\gamma^\xi} + H^f_{\pi\eta\omega\rho} \frac{\partial Y_\pi^{\eta f}}{\partial Y_\alpha^\beta}\frac{\partial Y_\omega^{\rho f}}{\partial Y_\gamma^\xi} + H^f_{\pi\eta\pi\eta} \frac{\partial Y_\pi^{\eta f}}{\partial Y_\alpha^\beta}\frac{\partial Y_\pi^{\eta f}}{\partial Y_\gamma^\xi} \tag{32}$$

Using Eq. (32) into Eq. (30) results is the consistent spreading of fibers contribution over the matrix properties, that is

$$H = H_s + H_f \tag{33}$$

The different values that $\frac{\partial Y_\pi^{\eta f}}{\partial Y_\gamma^\xi}$ assumes in Eqs. (32) depending on the adopted discretization, that is, the fibers, short or long in each lamina, may have the following settings related to the mid-surface of the plate or shell (see Fig. 4):

ISSN 2176-5480

both nodes of the fiber can be inserted in the same plate or shell finite element (fiber class 1), the nodes of the fiber may be in adjacent elements with $(GP+1)$ nodes in common (fiber class 2); the nodes of fiber may be in adjacent elements with just a node in common (fiber class 3) or, each node may be in finite elements not adjacent, i.e. without any node in common (fiber class 4).

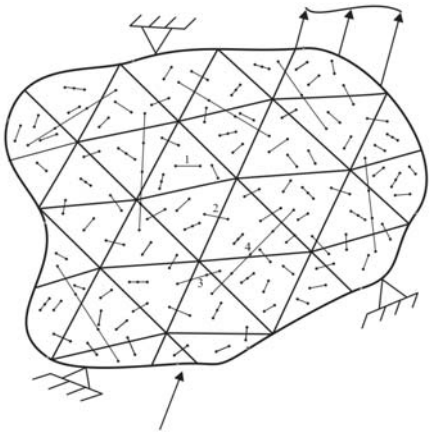

Figure 4. Mid-surface fibre-matrix discretization

To simplify the numerical procedure, the Hessian matrix of the fiber $[H^f]_{3(GP^f+1)x3(GP^f+1)}$ given in Eq. (27) is expanded into a matrix of order $7(GP^f+1)N \; x \; 7(GP^f+1)N$ by means of a sparse matrix $[\Psi]_{3(GP^f+1)x7(GP^f+1)N}$, as

$$\begin{aligned} H_f = \hat{H}_f &= [\hat{H}_f]_{7(GP^f+1)Nx7(GP^f+1)N} \\ &= [\Psi]^T_{7(GP^f+1)Nx3(GP^f+1)} \cdot [H^f]_{3(GP^f+1)x3(GP^f+1)} \cdot [\Psi]_{3(GP^f+1)x7(GP^f+1)N} \end{aligned} \tag{34}$$

where N is the number of nodes of the plate element and GP^f is the fiber approximation order.

For a fibre with GP^f+1 nodes the sparse matrix $[\Psi]$ is written as

$$[\Psi] = \begin{bmatrix} [\psi]_1 & 0 & 0 & 0 & 0 & 0 & 0 \\ 0 & [\psi]_2 & 0 & 0 & 0 & 0 & 0 \\ 0 & 0 & [\psi]_3 & 0 & 0 & 0 & 0 \\ 0 & 0 & 0 & \ddots & 0 & 0 & 0 \\ 0 & 0 & 0 & 0 & [\psi]_{N-2} & 0 & 0 \\ 0 & 0 & 0 & 0 & 0 & [\psi]_{N-1} & 0 \\ 0 & 0 & 0 & 0 & 0 & 0 & [\psi]_N \end{bmatrix}_{7(GPf+1)N \; x \; 3(GPf+1)} \tag{35}$$

Each term of the matrix $[\Psi]$ given in Eq. (35) is given by another matrix as shown below

$$[\psi]^P_\beta = \begin{bmatrix} \psi_{11} & 0 & 0 & \psi_{14} & \psi_{15} & 0 & 0 \\ 0 & \psi_{22} & 0 & \psi_{24} & 0 & \psi_{26} & 0 \\ 0 & 0 & \psi_{33} & \psi_{34} & 0 & 0 & \psi_{37} \end{bmatrix}_{3x7} \tag{36}$$

where β is the plate node and P is the fibre node that belong to the plate element.

To obtain the terms in Eq. (35) it is necessary differentiate Eq. (18) regarding a generic nodal plate coordinate. Remembering that $Y_4^k = \bar{T}^k$, $Y_5^k = \bar{G}_1^k$, $Y_6^k = \bar{G}_2^k$, $Y_7^k = \bar{G}_3^k$ the necessary derivatives are as follows

ISSN 2176-5480

$$\psi_{i(i)} = \frac{\partial Y_i^P}{\partial Y_{(i)}^{\beta f}} = \phi_\beta(\xi_1^P, \xi_2^P) \tag{37}$$

$$\psi_{i4} = \frac{\partial Y_i^P}{\partial Y_4^{\beta f}} = \left[\phi_\beta(\xi_1^P, \xi_2^P) \left(d^{lam} + \frac{h_0^{lam}}{2} \xi_3^P \right)^2 \right] \phi_k(\xi_1^P, \xi_2^P) Y_{i+4}^k \tag{38}$$

$$\psi_{i(i+4)} = \frac{\partial Y_i^P}{\partial Y_{(i+4)}^{\beta f}} = \left[\left(d^{lam(P)} + \frac{h_0^{lam(P)}}{2} \xi_3^P \right) + \phi_\ell(\xi_1^P, \xi_2^P) Y_4^\ell \left(d^{lam} + \frac{h_0^{lam}}{2} \xi_3^P \right)^2 \right] \phi_\beta(\xi_1^P, \xi_2^P) \tag{39}$$

with $i = 1,2,3$.

As we can see from Eqs. (37)-(39) the developed sparse matrix $[\Psi]$ given by Eq. (35) depends on the value of $\phi_\beta(\xi_1^P, \xi_2^P, \xi_3^P, d_{lam})$ and on which plate elements the fibre nodes P belong and the expanded fibre matrix $\hat{H}_f$ given by Eq. (34) is distributed over the total Hessian given in Eq. (30) following the plate nodal connectivity associated to belonging fiber nodes.

The procedure to find on which plate elements the fibre nodes belong is a simple and fast Newton-Raphson nonlinear solver and a detailed description about the fiber internal force and Hessian matrix spreading operation it was presented by (Sampaio *et al*., 2013).

6. THE EQUILIBRIUM PROBLEM SOLUTION PROCEDURE

In this section, the strategy adopted to solve the equilibrium problem of a laminate reinforced plate geometrically nonlinear is described. The non-linear analysis starts writing the total potential energy, for a conservative elastostatic problem, as

$$\Pi = U - \Omega \tag{40}$$

where Π is the total potential energy of the system, U is the strain energy including matrix and fiber contributions written regarding plate nodal positions and Ω is the potential energy of external conservative applied forces given by

$$\Omega = Y_j F_j \tag{41}$$

in which F_j is the vector of external forces and Y_j is the current position vector.

The Principle of Minimum Total Potential Energy (Tauchert, 1974) is applied writing the equilibrium equation as the derivative of total energy regarding nodal positions, plate for instance, as

$$g_j = \frac{\partial \Pi}{\partial Y_j} = \frac{\partial U}{\partial Y_j} - F_j = F_j^{int} - F_j = 0 \tag{42}$$

In Eq. (42) vector g_j assumes null value for the exact position and is the unbalanced mechanical residuum if a trial position solution is tested. From these considerations one writes the Newton-Raphson procedure as described by (Coda and Paccola, 2007; Coda and Paccola, 2008) for example.

7. NUMERICAL EXAMPLES

Two simple examples are shown in order to demonstrate the good behavior of the proposed formulation. The first one is used to confirm that the mechanical coupling between fibers and the laminated shell element is working properly during large displacement analyses. The second one deals with a simple supported reinforced square plate.

7.1 Clamped beam - large displacement

In this example we analyze a simply clamped beam requested by a uniformly distributed load q. The beam is enhanced by four stiffeners disposed as shown in Fig. 5. We compare the displacement achieved with the proposed formulation (composite formulation) with three different formulations: a) the Timoshenko-Reissner 3D beam formulation presented in (Coda and Greco, 2004; Coda, 2009; Coda and Paccola, 2010; Coda and Paccola, 2011), b) a

ISSN 2176-5480

fibre-matrix 2D solid formulation presented in (Sampaio *et al.*, 2013), and c) a laminated shell formulation presented in (Coda *et al.*, 2013). The geometrical properties adopted for the beam are as follows: $L = 300cm$, $b = 20cm$, $h = 60cm$, $d = 3cm$ and $q = 5.0MN/m$. The Young modulus and the Poisson ration of the matrix are $E_m = 21GPa$ and $\nu = 0$, respectively, while Young´s modulus and cross-sectional area of each fibre are $E_f = 210GPa$ and $A_f = 2cm^2$, respectively. When using the proposed formulation (composite), the laminated formulation and the 2D solid formulation, the matrix is discretized into 60 cubic solid elements with a total of 364 nodes. Each reinforcement is discretized into 30 cubics fibre elements. The 3D frame element analysis employs 10 fifth order elements.

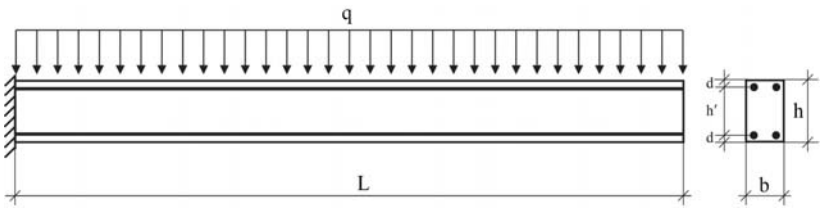

Figure 5. Fibre reinforced cantilever beam

Figure 6 shows the final deformed shapes and Fig. 7 compares the displacements achieved for the different formulations.

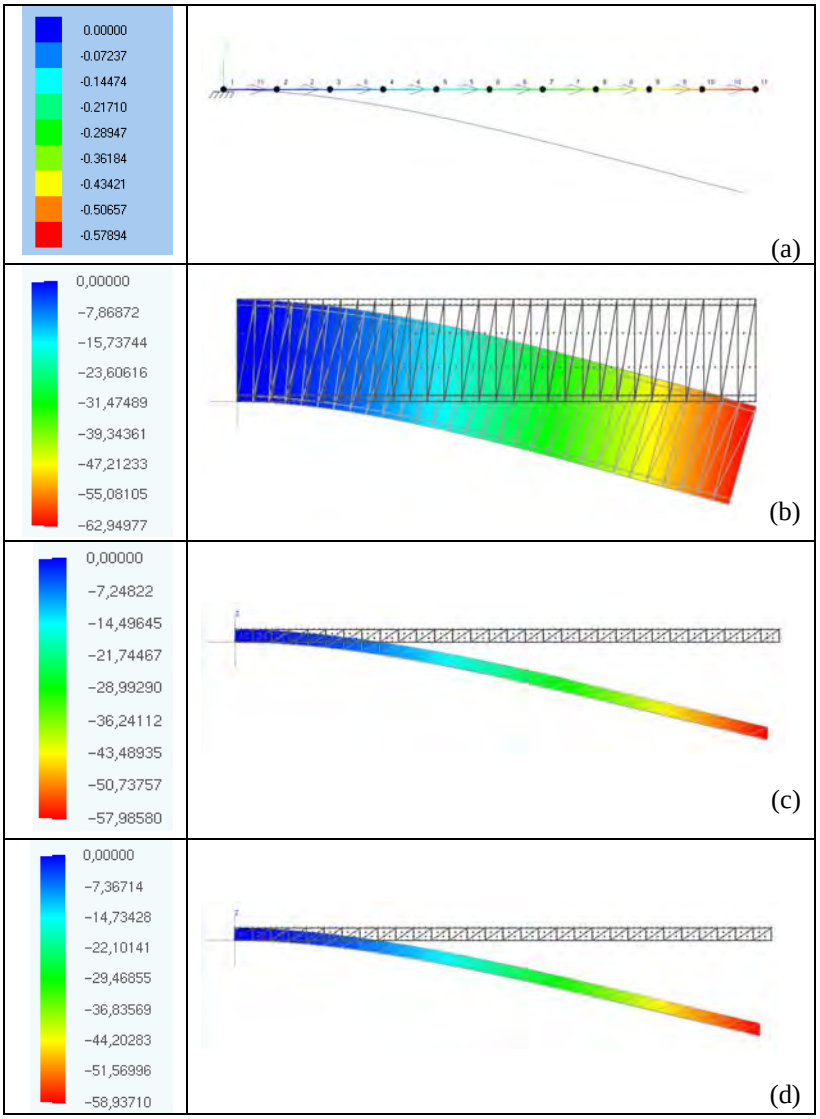

Figure 6. Transverse displacements of the beam: (a) 3D frame solution in (m); (b) 2D solid solution in (cm); (c) laminated equivalent solution in (cm); (d) composite solution in (cm).

ISSN 2176-5480

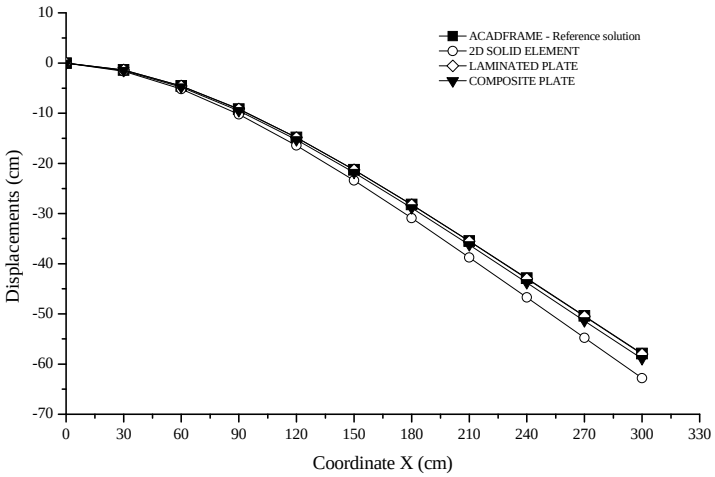

Figure 7. Transverse displacement of the beam (cm)

The maximum deflection in the free end of the reinforced beam as well the relative difference between the different formulations related to reference solution (3D Frame) are shown in Table 1. The composite formulation is more flexible than the laminated formulation as expected. The great relative difference presented by 2D solid formulation is because the Timoshenko-Reissner solution presents more kinematics restrictions. This results indicates the appropriateness of the proposed formulation for large displacement analysis.

Table 1. Numerical values of the maximum transverse displacement (cm).

3D FRAME (REFERENCE SOLUTION)	2D SOLID	PLATE	
		LAMINATED	COMPOSITE
-57,894	-62,823	-57,985	-58,937
Relative difference	~7,84%	~0,15%	~1,76%

7.2 Simple supported reinforced square plate

In this example a simple supported square plate with $L = 400cm$ and $h = 16cm$ under a uniform distributed load ($q = -1.0kN/m^2$) is analyzed, Fig. 8. We compare the results achieved with the proposed formulation with the laminated shell formulation. Two cases are considered: isotropic plate and orthotropic plate. For the isotropic material the Young modulus and the Poisson ration of the plate are $E_p = 21GPa$ and $\nu = 0.25$. In the laminated formulation (orthotropic case) we assume $E_{11} = 210GPa$, $E_{22} = E_{33} = 21GPa$ and $\nu = 0$. When using the proposed formulation the Young modulus and cross-sectional area of each fibre are $E_f = 210GPa$ and $A_f = 2cm^2$, respectively.

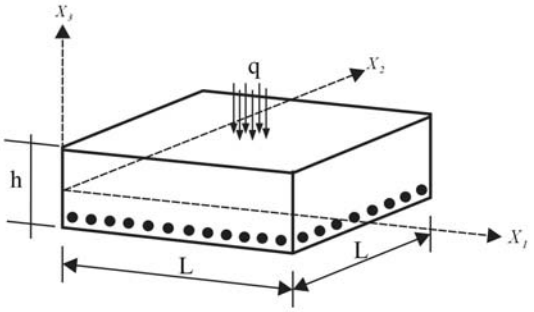

Figure 8. Simple supported reinforced square plate

For all analysis only a quarter of the problem has been discretized by 10 x 10 regular mesh with 200 cubic triangular elements and 961 nodes, see Fig. 9a. For the isotropic plate, each direction have 20 long fibres disposed each 10 cm.

ISSN 2176-5480

Each reinforcement is discretized into 10 cubics fibre elements, Fig. 9b. For the orthotropic plate we have 20 long fibres each 10cm discretized into 10 cubics fibre elements, Fig. 9c.

(a) (b) (c)

Figure 9. Mesh of a quarter of the problem: (a) matrix; (b) fibres for isotropic plate; (c) fibres for orthotropic plate

Figure 10 shows the transverse displacement of the plate and Table 2 shows the central displacement for the different analysis.

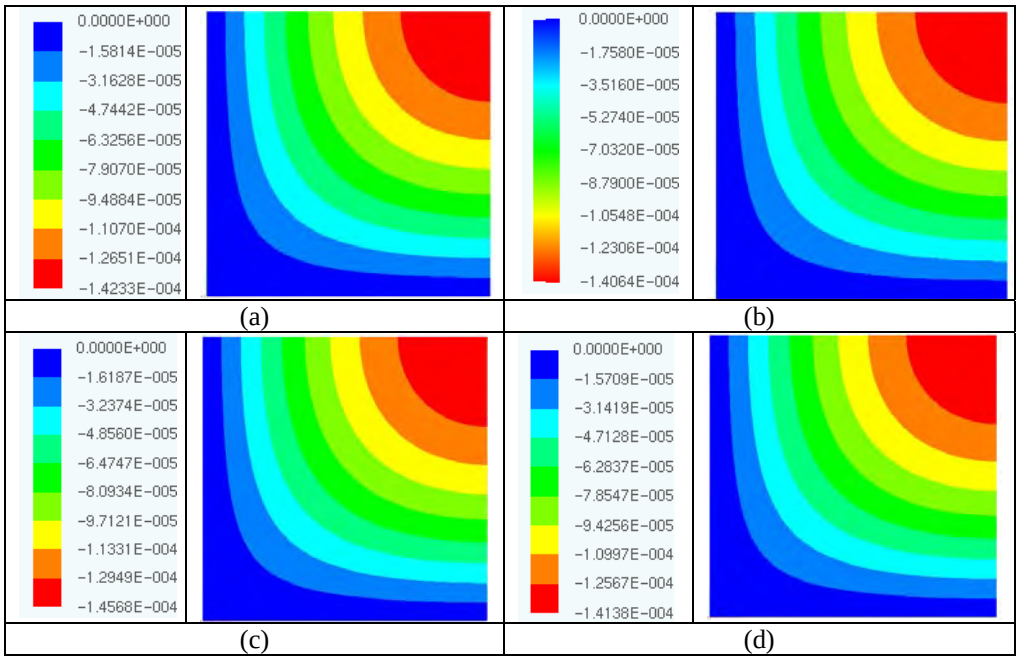

Figure 10. Transverse displacement of a quarter of the problem: (a) isotropic laminated; (b) isotropic composite; (c) orthotropic laminated; (d) orthotropic composite.

Table 2. Numerical values of the maximum transverse displacement in (m).

HOMOGENEOUS PLATE	ISOTROPIC		ORTHOTROPIC	
	LAMINATED	COMPOSITE	LAMINATED	COMPOSITE
-1.5680×10^{-4}	-1.4233×10^{-4}	-1.4064×10^{-4}	-1.4568×10^{-4}	-1.4138×10^{-4}

As we can see from Table 2 the results are as expected, that is, the maximum transverse displacement obtained for the isotropic plate are less flexible than the homogeneous plate and the orthotropic plate solutions are more flexible than the isotropic solution indicating the good behavior of the proposed formulation.

8. CONCLUSION

In this paper we introduced a strategy to insert fibres, shorts or longs, in laminated plates or shells finite elements for the geometrically non-linear analyses. This strategy does not increase the number of degrees of freedom and its main advantage is because the fibre reinforced laminates are usually analyzed by homogeneous analog which makes difficult

ISSN 2176-5480

to identify the contact stresses between fibres and matrix. As we can see from presented applications, the values are coherent and as expected demonstrating the good behavior of our strategy. We future words we intend present a way to calculate the contact stresses.

9. ACKNOWLEDGEMENTS

This research is supported by CAPES (Brazil), Amazonas Research Foundation (FAPEAM) and São Paulo Research Foundation (FAPESP).

10. REFERENCES

Bolander Jr., J.E., Saito, S., 1997. “Discrete modeling of short-fiber reinforcement in cementitious composites”, Advanced Cement Based Materials 6, 76–86.

Ciarlet, P.G., 1993. “Mathematical Elasticity”. North-Holland.

Chudoba, R., Jerábek, J., Peiffer, F., 2009. “Crack-centered enrichment for debonding in two-phase composite applied to textile reinforced concrete”, International Journal for Multiscale Computational Engineering, 7(4), 309–328.

Coda, H.B., Greco, M., 2004. A simple FEM formulation for large deflection 2D frame analysis based on position description, Comput. Methods Appl. Mech. Eng. 193 (33–35), 3541–3557.

Coda, H.B., Paccola, R.R., 2007. “An alternative positional FEM formulation for geometrically non-linear analysis of shells: Curved triangular isoparametric elements”, Computational Mechanics, 40(1), 185-200.

Coda, H.B., Paccola, R.R., 2008. “A positional FEM Formulation for geometrical non-linear analysis of shells”, Latin American Journal of Solids and Structures, 5, 205-223.

Coda, H.B., 2009. A solid-like FEM for geometrically non-linear 3D frames, Comput. Methods Appl. Mech. Eng. 198 (47-48), 3712–3722.

Coda, H.B., Paccola, R.R., 2010. Improved finite element for 3D laminate frame analysis including warping for any cross-section, Appl. Math. Model. 34 (4), 1107–1137.

Coda, H.B., Paccola, R.R., 2011. A. FEM, procedure based on positions and uncon- strained vectors applied to non-linear dynamic of 3D frames, Finite Elem. Anal. Des. 42 (4), 319–333.

Coda, H.B., Paccola, R.R., Sampaio, M.S.M., 2013. “Positional description applied to the solution of geometrically non-linear plates and shells”, Finite Analysis and Design, 67, 66-75.

Hettich, T., Hund, A., Ramm, E., 2008. “Modeling of failure in composites by X-FEM and level sets within a multiscale framework”, Computer Methods in Applied Mechanics and Engineering, 197, 414-424.

Hyer, M.W., 1997. “Stress Analysis of fiber-reinforced Composite Materials”, McGraw-Hill Publ., New York, 627 p., 1997.

Luenberger, D.G., 1989. “Linear and nonlinear programming”, Addison-Wesley Publishing Company.

Melenk, J.M., Babuska, I., 2006. “The partition of unity finite element method: basic theory and applications”, Computer Methods in Applied Mechanics and Engineering, 139, 289–314.

Ogden, R.W., 1984. “Non-linear Elastic deformation”, Ellis Horwood, England.

Oliver, J., Linero, D.L., Huespe, A.E., Manzoli, O.L., 2008. “Two-dimensional modeling of material failure in reinforced concrete by means of a continuum strong discontinuity approach”, Computer Methods in Applied Mechanics and Engineering, 197, 332–348.

Radtke, F.K.F., Simone, A., Sluys, L.J., 2011. “A partition of unity finite element method for simulating nonlinear debonding and matrix failure in thin fibre composites”, Int. J. Numer. Meth. In Engrg., 86(4-5), 453-476.

Radtke, F.K.F., Simone, A., Sluys, L.J., 2010a. “A partition of unity finite element method for obtaining elastic properties of continua with embedded thin fibres”, Int. J. Numer. Meth. In Engrg., 84(6), 708-732.

Radtke, F.K.F., Simone, A., Sluys, L.J., 2010b. “A computational model for failure analysis of fibre reinforced concrete with discrete treatment of fibres”, Engineering Fracture Mechanics, 77(4), 597-620.

Sampaio, M.S.M., Paccola, R.R., Coda, H.B., 2013. “Fully adherent fiber-matrix FEM formulation for geometrically nonlinear 2D solid analysis”, 66, 12-25.

Schlangen, E., Mier, J.G.M., 1992. “Simple lattice model for numerical simulation of fracture of concrete materials and structures”, Materials and Structures 25, 534–542.

Tauchert, T.R., 1974. “Energy principles in structural mechanics”, McGraw Hill.

11. RESPONSIBILITY NOTICE

The authors are the only responsible for the printed material included in this paper.